

ORIGINAL ARTICLE Neuro/Head and Neck Radiology

Pseudoexfoliation syndrome: Gray matter volume and microstructural changes revealed by histogram and brain surface analysis

Christos V. Gkizas¹, Loukas G. Astrakas², Anastasia K. Zikou¹, Vasileios G. Xydis¹, George Kitsos³, Maria I. Argyropoulou¹

¹Department of Radiology, Faculty of Medicine, University of Ioannina, Greece

²Department of Medical Physics, Faculty of Medicine, University of Ioannina, Greece

³Department of Ophthalmology, Faculty of Medicine, University of Ioannina, Greece

SUBMISSION: 27/4/2020 - ACCEPTANCE: 23/6/2020

ABSTRACT

Purpose: White matter (WM) abnormalities may occur in patients with pseudoexfoliation syndrome (PXS). The presence of gray matter (GM) abnormalities in patients with PXS without glaucoma was evaluated, applying histogram and brain surface analysis of MRI data.

Material and Methods: Brain MRI was conducted on 20 patients newly diagnosed with PXS without glaucoma, (mean age 68.7 ± 8.6 years) and 14 control subjects (mean age 63.3 ± 6.6 years). The histogram scalars of mean diffusivity (MD) and fractional anisotropy (FA) of GM and WM were evaluated. Brain surface analysis was performed on 3D T1-weighted images.

Results: The MD value of the WM showed higher mean, standard deviation, median and 75th percentile in the patients than in the control subjects. The FA values of GM showed higher mean, standard deviation, median and 75th percentile, and lower kurtosis and skewness in the patients than in the control subjects. Greater GM volume was observed in the patients in Brodmann areas 25 and 26.

Conclusions: Patients with PXS may present microstructural changes of the GM that could be associated with the deposition of extracellular fibrillar material and increased cortical volume in areas related to depression.



CORRESPONDING
AUTHOR,
GUARANTOR

Maria I Argyropoulou
Department of Radiology, Faculty of Medicine, School of Health Sciences
University of Ioannina, P.O. Box 1186, 45110 Ioannina, Greece,
Email: margyrop@cc.uoi.gr



KEY WORDS

Pseudoexfoliation syndrome; Diffusion tensor imaging; Histogram analysis; Cortical surface analysis; MR imaging; Brain

Introduction

Pseudoexfoliation syndrome (PXS) is a systemic age-related microfibrilopathy characterised by the production and deposition of extracellular fibrillar material (EFM) in the eye, meninges, blood vessels and visceral organs [1]. The prevalence of PXS differs between various population groups, depending on genetic and environmental factors [2]. Slit lamp examination of the eye reveals whitish, flaky amyloid-like deposits on the anterior segment structures, particularly on the anterior surface of the lens and the pupillary border of the iris, which represent the clinical hallmark of the syndrome [1-3]. Involvement of the trabecular meshwork impairs drainage of aqueous humour from the anterior chamber and leads to increased intraocular pressure and development of pseudoexfoliative open-angle glaucoma (PEXG), with optic nerve damage and visual field loss [1-3]. Deposition of EFM in the vascular wall, leading to decreased elasticity and hypoperfusion, is associated with cardiovascular disease and stroke [2-5]. Doppler studies show decreased flow velocity and increased resistive index in the middle cerebral artery and single-photon emission computed tomography (SPECT) shows hypoperfusion in the frontal, temporal and parietal cortex [4-6]. White matter (WM) hyperintensities on T2-weighted (T2W) and FLAIR MR images, suggestive of brain vascular disease, have been reported in two studies of patients with PXS [6, 7], in one of which diffusion tensor imaging (DTI) revealed increased mean diffusivity (MD), radial diffusivity (RD) and axial diffusivity (AD) in major WM tracts and decreased fractional anisotropy (FA) in the optic tracts [7]. DTI has been largely used for the evaluation of WM microstructure in the brain and DTI metrics (MD, RD, AD, and FA) have been studied in normal maturing brain, in ageing and in various different disease processes [8]. There is an increasing interest in evaluating grey matter (GM) with DTI, for which ROI analysis and voxel wise techniques have been applied [9-12], which offer region specific information but are less effective in detecting slight and diffuse changes in GM and WM. Histogram analysis, by

evaluating the whole GM and/or WM, provides a non-invasive assessment of widespread, randomly distributed lesions and reveals subtle changes [13-18]. A histogram, which represents the distribution of voxel values and is described by scalars, is useful for characterisation of tissues and comparison between groups of patients and between patients and control subjects [13-18]. Descriptive scalars typically used are mean, standard deviation (SD), mode, maximum and minimum, kurtosis, skewness and percentiles. Histogram analysis avoids bias from disease location and therefore eliminates the need to preselect a region of interest (ROI). In serial or multi-subject studies and in multiple modalities it avoids registration problems which are particularly challenging in DTI data [13-18]. Histogram analysis has been used in the evaluation of age-related changes of brain microstructure, multiple sclerosis (MS), neurodegenerative and neuropsychiatric disorders, autoimmune disorders and brain tumours [13-18].

Based on the documented involvement of PXS in the blood vessels and meninges of the brain and the associated WM microstructural abnormalities, we applied histogram analysis of the two most common DTI metrics (i.e. fractional anisotropy and mean diffusivity) of the GM and the WM in patients with PXS without glaucoma. Our main hypothesis was that histogram analysis of DTI data obtained with a standard clinical pulse sequence using a 1.5T MRI scanner could reveal not only WM abnormalities in PXS, but also GM changes undetectable with other techniques. Based on the results of histogram analysis of GM microstructure we further applied surface analysis to investigate for regional cortical changes in volume, thickness and surface area.

Material and Methods

The study included 20 patients newly diagnosed with PXS, (11 females and 9 males; mean age \pm SD 68.7 ± 8.6 years) and 14 control subjects (10 females and 4 males; mean age 63.3 ± 6.6 years). All the patients fulfilled the diagnostic criteria for PXS established by the Amer-

ican Academy of Ophthalmology, which include the presence of light gray flakes on the anterior segment structures of the eye, (i.e. the corneal endothelium, iris, pupillary margin, lens capsule, and vitreous face), confirmed by pupil dilation and slit-lamp examination.

The study excluded patients with any form of cataract and PEXG or any other type of glaucoma (open angle, acute, congenital). Patients with clinical depression, antidepressant treatment, demyelinating disease, autoimmune disease, cardiovascular disease, peripheral artery disease, diabetes mellitus (DM) and hypertension (i.e. arterial blood pressure >140/90 mm Hg, or use of antihypertensive medications) were excluded also, in order to avoid marked impact on DTI. Other exclusion criteria were ophthalmic surgery, prior orbital trauma, optic nerve atrophy, diabetic retinopathy, cystoid macular oedema, age-related macular degeneration, uveitis, refractive errors in myopia or hypermetropia (>3.00 diopters) and astigmatism (>1.00 diopters).

All the participants were informed about the study and the procedure, and provided written consent. Those with a score of less than 23 on the mini-mental state examination, indicative of cognitive impairment, were excluded from the study.

The study was approved by the University Hospital of Ioannina Review Board and the Hospital Ethics Committee.

Clinical examination

All the study subjects underwent complete ophthalmological examination, including visual acuity (optotype Snellen), intraocular pressure measurement (Goldmann tonometer), gonioscopy, funduscopy with evaluation of the C/D, by using the Discam imaging system (Marcher Enterprises, Hereford, UK), assessment of visual fields (Humphrey, 24-2: mean deviation, PSD), and quantification of the retinal nerve fibre layer thickness (RNFLT) using Stratus OCT 3, Version 4 (Carl Zeiss, San Diego, California). Before the optical coherence tomography (OCT) scan, all participants were subjected to pupillary dilation with 0.5% tropicamide and 0.5% phenylephrine. They then underwent optic disc scanning, using the fast RNFLT protocol, which compresses the 3 sequential circular scans of 3.4-mm radius of the RNFLT protocol into 1 scan, performed in 1.92 seconds. The average RNFLT was extracted from the fast RNFLT

protocol at a distance of 3.4 mm from the center of the optic disc, for each of the 4 peripupillary quadrants (inferior, superior, nasal, and temporal). The universal RNFLT (mean RNFLT score for all quadrants) was also recorded.

Imaging

Diffusion data were collected using a 1.5-T scanner (Intera, Philips Medical Systems, Best, The Netherlands) and an eight-channel phased-array coil. The imaging protocol consisted of: 1) an axial T2-weighted (T2W) turbo spin-echo (TR, 3500 ms; TE, 120 ms; FOV, 230 mm; matrix, 256×256; slice thickness, 5 mm; intersection gap, 0.5 mm); 2) a sagittal T2W FLAIR sequence (TR, 6300 ms; TE, 120 ms; FOV, 250 mm; matrix, 256×256; slice thickness, 6 mm; intersection gap, 0.6 mm); 3) a T1-weighted (T1W) high-resolution (1×1×1 mm) 3D spoiled gradient-echo sequence (TR, 25 ms; TE, 4.6 ms; FOV, 220 mm); 4) a spin echo single shot EPI sequence (TE=131 ms; TR=9825 ms; FOV, 230 mm; matrix, 112×128; slice thickness, 3 mm; slice gap, 0 mm; 15 gradient directions with $b=1000$ s/mm² and one with $b=0$ s/mm²).

Histogram Analysis

Diffusion DICOM images were converted into gzipped NIfTI-1.1 [.nii.gz] format using the dcm2nii tool of MRICron (<http://www.mccauslandcenter.sc.edu/mricron/>). All the images were then analysed using tools from the FMRIB Software Library (FSL). The diffusion images were corrected for head motion and eddy current induced distortion and then a brain mask was created using the brain extraction tool on the $b=0$ image. Finally, MD and FA maps were calculated using DTIFIT, applying a diffusion tensor model to each voxel.

For each subject the T1W image was registered on the $b=0$ images and then it was a segment, producing GM and WM probability images in the subject's native space. A 0.5 threshold was imposed on these images to create GM and WM binary masks, which were used to segment FA and MD maps into GM (FAgm, MDgm, respectively) and WM (FAwm, MDwm, respectively) parts.

An in-house developed MATLAB script was used to calculate histograms and metrics i.e., mean, SD, median, mode, kurtosis, skewness, 25th percentile (prctile25), 75th percentile (prctile75), for each of the FAwm,

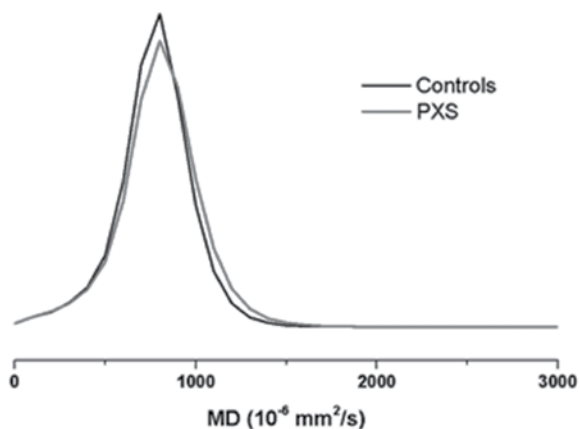


Fig 1. White matter mean diffusivity (MDwm) average histograms of patients with (PXS) and control subjects.

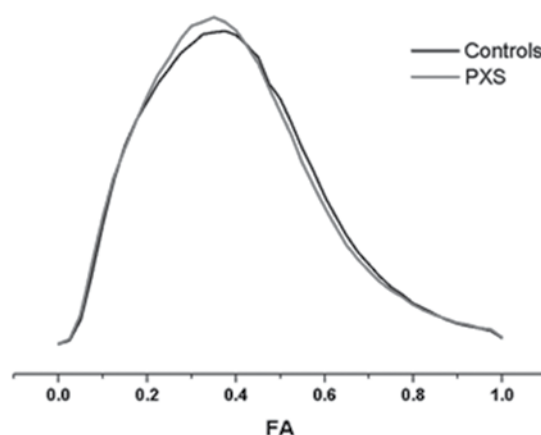


Fig 2. White matter fractional anisotropy (FAwm) average histograms of patients with (PXS) and control subjects.

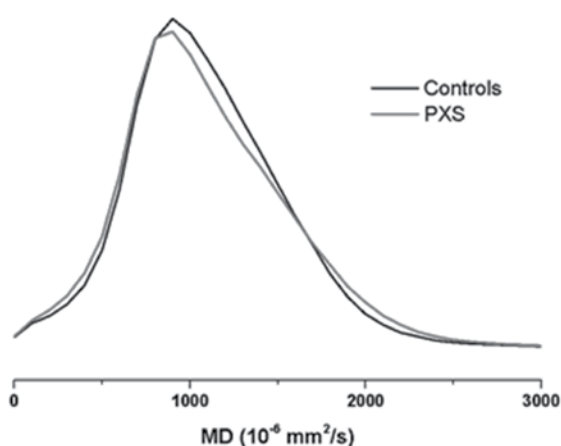


Fig 3. Gray matter mean diffusivity (MDgm) average histograms of patients with (PXS) and control subjects.

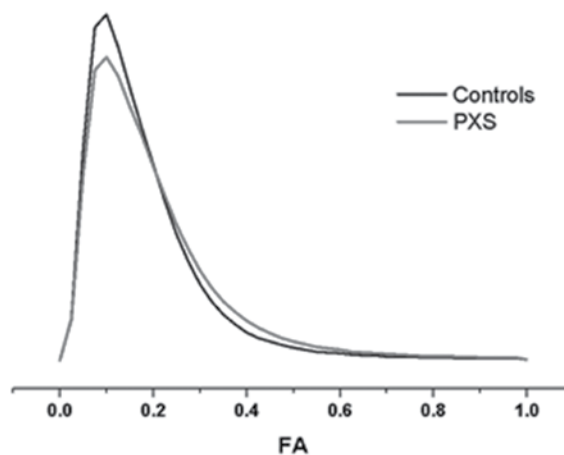


Fig 4. Gray matter fractional anisotropy (FAgm) average histograms of patients with (PXS) and control subjects.

MDwm, FAgm, MDgm, maps. After normality testing the Mann Whitney U test was used to detect differences in the histogram indices between patients and control subjects. Average histograms of MD and FA values of WM and GM maps were calculated and plotted for patients and control subjects.

Multivariate stepwise forward logistic regression was performed to identify independent predictors of PXS among the histogram metrics. Multicollinearity was assessed using the variance inflation factor (VIF). Age and sex were included as covariates in the regression model

to control for their possible confounding effects.

Cortical Surface Analysis

Cortical surface analysis of the T1-weighted images was employed using the FreeSurfer image processing pipeline developed especially for infant clinical MRI images. Surface analysis provided for each subject and for each hemisphere maps of cortical thickness and cortical area. Group comparison of each map was performed at the ROI level after parcellating each brain using the Brodmann atlas PALS12. The mean values of area,

Table 1. White matter mean diffusivity histogram indices in patients with pseudoexfoliation syndrome (PXS) patients and control subjects

	Control subjects	PXS	P value (Mann Whitney U Test)
	Median [Min, Max]	Median [Min, Max]	
mean	772 [739, 7798]	802 [718, 878]	0.023
SD ^a	208 [197, 256]	227 [192, 289]	0.039
median	776 [752, 813]	830 [730, 883]	0.027
mode	809 [627, 879]	842 [741, 981]	0.077
kurtosis	7.6 [4.8, 10.4]	6.7 [4.7, 13.6]	0.097
skewness	0.18 [-0.19, 4.39]	0.12 [-0.23, 0.63]	0.592
prctile25 ^b	662 [603, 687]	677 [603, 765]	0.192
prctile75 ^b	888 [856, 951]	932 [648, 1020]	0.008

All variables except kurtosis and skewness have standard diffusion units $10^{-6}\text{mm}^2/\text{s}$.

^aSD=standard deviation, ^bprctile=percentile

thickness, volume and curvature in the Brodmann areas (BA) of the surface maps were compared between patients and controls using the Mann-Whitney U-test combined with Bonferonni correction for multiple comparisons differences. Statistical analysis was performed using the IBM SPSS software package, version 23.0 (IBM Corporation, Armonk, NY). A two-tailed threshold of $P<0.05$ was used for statistical significance.

Results

Average MDwm histograms (**Fig. 1**) show more voxels in the high MD range ($>750*10^{-6}\text{mm}^2/\text{s}$) in the patients, and more voxels in the low MD range ($<750*10^{-6}\text{mm}^2/\text{s}$) in the control subjects. Group analysis of MDwm values showed higher mean, median and prctile75 values in the patients than in the control subjects (**Table 1**). Average FAwm histograms of patients and control subjects are almost identical (**Fig. 2**) and statistical analysis revealed no significant differences in their metrics (**Table 2**). Average MDgm histograms (**Fig. 3, Table 3**) showed no differences between patients and control subjects. The average FAGm histogram (**Fig. 4**) of patients was less populated around the peak and more populated in the tails, especially in the right tail. Group analysis of FAGm values showed higher mean, median

and prctile75 and lower kurtosis and skewness in the patients than in the control subjects (**Table 4**).

Logistic regression analyses showed that among the histogram metrics the only predictors of PXS were prctile75 ($P=0.023$, $VIF=1.031$) of the MDwm distribution and the mean FAGm distribution ($P=0.018$, $VIF=1.028$).

Cortical surface analysis showed that patients had larger volume than controls at the Brodmann areas 25 ($P=0.006$) and 26 ($P=0.009$) of the right hemisphere.

Discussion

The major findings of this study were increased diffusivity of WM, increased anisotropy of GM and greater cortical volume in Brodmann areas 25 and 26, in the patients with PXS. FA describes the degree of anisotropy of diffusion and MD is a measure of the average diffusivity of water molecules within a voxel [8]. The histogram scalars used were mean, SD, mode, kurtosis, skewness and percentiles. The mean describes the average of voxel values, SD the dispersion of voxel values, mode the voxel value with the highest counts, kurtosis the peakedness of the histogram and skewness the degree of its asymmetry. A percentile represents the voxel value below which a percentage (25%, 50% or median and 75%) of voxel values are found [10].

Table 2. White matter fractional anisotropy histogram indices in patients with pseudoexfoliation syndrome (PXS) and control subjects.

	Control subjects	PXS	P value (Mann Whitney U Test)
	Mean [Min, Max]	Mean [Min, Max]	
mean	0.40 [0.37, 0.42]	0.39 [0.35, 0.44]	0.290
SD ^a	0.18 [0.19, 0.19]	0.17 [0.19, 0.20]	0.823
median	0.38 [0.34, 0.41]	0.37 [0.33, 0.42]	0.259
mode	0.36 [0.27, 0.36]	0.36 [0.26, 0.36]	1.000
kurtosis	2.93 [2.72, 3.37]	3.12 [2.69, 3.65]	0.129
skewness	0.52 [0.37, 0.79]	0.61 [0.42, 0.82]	0.120
prctile25 ^b	0.26 [0.23, 0.28]	0.25 [0.22, 0.30]	0.436
prctile75 ^b	0.51 [0.47, 0.55]	0.50 [0.46, 0.56]	0.245

^aSD=standard deviation, ^bprctile=percentile

Table 3. Gray matter mean diffusivity histogram indices in patients with pseudoexfoliation syndrome (PXS) and control subjects.

	Control subjects	PXS	P value (Mann Whitney U Test)
	Median [Min, Max]	Median [Min, Max]	
mean	0.40 [0.37, 0.42]	0.39 [0.35, 0.44]	0.290
SD ^a	0.18 [0.19, 0.19]	0.17 [0.19, 0.20]	0.823
median	0.38 [0.34, 0.41]	0.37 [0.33, 0.42]	0.259
mode	0.36 [0.27, 0.36]	0.36 [0.26, 0.36]	1.000
kurtosis	2.93 [2.72, 3.37]	3.12 [2.69, 3.65]	0.129
skewness	0.52 [0.37, 0.79]	0.61 [0.42, 0.82]	0.120
prctile25 ^b	0.26 [0.23, 0.28]	0.25 [0.22, 0.30]	0.436
prctile75 ^b	0.51 [0.47, 0.55]	0.50 [0.46, 0.56]	0.245

^aSD=standard deviation, ^bprctile=percentile

The MD values of the WM of the patients with PXS showed higher mean, SD, median and prctile75, the latter being identified as a predictor of PXS. Median (prctile50) represents the intermediate and prctile75 the higher values of MD and their concurrent changes show involvement of a large number of voxels. Over-

all, for the largest part of WM, diffusivity became more heterogeneous and unrestricted. This is in agreement with a previous study on PXS which on analysis of DTI data with TBSS revealed increased MD, AD and RD in the anterior thalamic radiation, inferior fronto-occipital fasciculus, superior longitudinal fasciculus, in-

Table 4. Gray matter fractional anisotropy histogram indices in patients with pseudoexfoliation syndrome (PXS) and control subjects.

	Control subjects	PXS	P value (Mann Whitney U Test)
	Median [Min, Max]	Mean [Min, Max]	
mean	0.18 [0.15, 0.20]	0.19 [0.18, 0.25]	0.011
SD ^a	0.13 [0.12, 0.16]	0.15 [0.13, 0.20]	0.006
median	0.15 [0.12, 0.16]	0.16 [0.14, 0.21]	0.023
mode	0.16 [0.06, 0.16]	0.16 [0.05, 0.16]	0.231
kurtosis	10.36 [8.06, 16.05]	9.45 [4.08, 11.92]	0.009
skewness	2.19 [1.89, 3.04]	2.10 [1.25, 2.51]	0.050
prctile25 ^b	0.09 [0.08, 0.11]	0.10 [0.09, 0.14]	0.129
prctile75 ^b	0.23 [0.18, 0.25]	0.24 [0.22, 0.36]	0.023

^aSD=standard deviation, ^bprctile=percentile

ferior longitudinal fasciculus and forceps minor [7]. Marked increase in MD has been associated with direct WM injury, while a slight increase is observed in secondary degeneration (Wallerian degeneration) of the WM fibers [19]. Hypoperfusion of the brain has been reported in patients with PXS, and EFM deposition in the vascular wall is considered responsible for the development of degenerative fibrillopathy and decreased vessel compliance [2-6]. Chronic hypoperfusion of the brain may lead to apoptotic cell death of oligodendrocytes, due to oxidative stress with production of free radicals and proinflammatory cytokines [20-23]. The normal myelination process depends on normal oligodendrocytes and thus hypoperfusion may result in demyelination and axonal damage. The prctile25, which represents the lowest voxel values of MD, showed no difference between the patients and the control subjects. Low values of MD have been found in areas with crossing WM fibers, which show a decreased diffusivity from an increase in tissue compactness [24, 25]. The lack of MD change in those areas could be related to the development of gliosis which would counterbalance fiber loss, or it may be that fiber loss is not so important for changing tissue compactness as measured by MD. Absence of change in the FA of WM was observed, in agreement with a previous study, suggesting that diffu-

sion was decreased equally along the three eigenvalues and anisotropy remained unaffected [7]. The present study showed that degeneration with increased diffusivity of extensive areas of WM appears to be a significant predictor of PXS.

Detectable anisotropy of the normal GM is only observed between 24-32 weeks of gestation, at which stage it is due to the presence and parallel disposition of the radial glial fibers participating in the neuronal migration process [26]. GM of the adult brain has not been extensively studied with diffusion techniques because it is an almost isotropic structure presenting very low FA values. In this study the FA values of GM showed higher mean, SD, median and prctile75 and lower kurtosis and skewness in patients than in control subjects. The median and prctile75 taken together represent the largest part of voxel values and their increase creates a shift in the mean FA towards higher values. The lower kurtosis and skewness and the higher SD are due to displacement of the voxel values towards the tails, and especially the right tail. Overall, in patients with PXS the GM becomes more anisotropic. Two possible underlying mechanisms for this increase in anisotropy in GM are suggested: 1) In PXS, the deposition of EFM has been found not only in the wall of brain vessels but also in the arachnoid villi and me-

ninges [1-3]. Brain arteries penetrating and vascularising the GM are surrounded by the perivascular Virchow Robin (VR) spaces, formed by a single pia layer in the cortex and a double pia layer in the subcortical GM [27, 28]. Deposition of EFM on these leptomeningeal layers, following the architectural disposition of vessels, might provide anisotropy and increase the FA of the GM, or 2) major WM tracts connect cortical and subcortical areas of the brain and short WM fibers serve for intrinsic cortical and subcortical connections [25]; in PXS hypoperfusion related degeneration of major WM fibers, along with a relative preservation of the intra cortical and subcortical anisotropic short WM fibers, might be responsible for the increase in FA [7, 29].

In this study the mean FA of the GM was an important predictor of PXS, indicating the value of assessing anisotropy in GM. Of the various DTI metrics, MD is considered the most reliable for the evaluation of the relatively isotropic GM. No changes were observed in the MD of GM. Two opposing processes, the one decreasing and the other increasing, compactness, such as degeneration of major WM fibers connecting the cortex with the subcortical GM in combination with deposition of EFM along the wall of the perivascular VR spaces, might be responsible for this lack of difference between patients and control subjects.

Brodmann areas 25 and 26 are part of the cingulate gyrus, which has been associated with depression [30]. Increased depression scores have been reported in patients with PXS and glaucoma, but no relevant imaging studies have been performed [31]. The present MRI study in patients with PXS without glaucoma or clinical depression demonstrated increased cortical volume of Brodmann areas 25 and 26. Previous studies in patients with subthreshold depressive symptoms have demonstrated increased cortical volume in subregions of the cingulate gyrus, while in those with clinical depression, decreased volume and increased activation of the same areas were reported [30, 32]. Particularly, the human area 25 has received significant attention in the context

of negative emotions and anhedonia [33]. As current classification systems are based on subjective descriptions of symptoms, the study subjects were not examined for subthreshold depression. It is possible that in the patients studied here, increased cortical volume of subregions of the cingulate gyrus might not only herald the future development of clinical depression but also a prodromal indicator for subsyndromal depression and/or anhedonia.

The main limitations of this cross-sectional study are the small number of patients and the 1.5 T field strength of the MRI. Future more populated studies, with higher magnetic fields, would be useful to validate the potential of structural MRI for improving our understanding of the mechanisms by which PXS affects the brain.

In conclusion, histogram analysis reveals predominant microstructural changes in WM and an abnormal anisotropic appearance of GM in patients with PXS. Demyelination and axonal degeneration might be the anatomical substrate of the WM abnormalities. EFM deposition and degeneration of the major WM tracts, associated with short WM fiber preservation, is the suggested cause of GM abnormalities. Increased volume in subregions of the cingulate gyrus might represent a prodromal finding for future development of depression. **R**

Abbreviations

EFM=extracellular fibrillar material; FA=fractional anisotropy; MD=mean diffusivity; Prctile=percentile; PEXG=pseudoexfoliative open-angle glaucoma; PXS=pseudoexfoliation syndrome

Funding

This project did not receive any specific funding.

Ethical approval

The University Hospital of Ioannina Ethics Committee.

Conflict of interest

The authors declared no conflicts of interest.

REFERENCES

1. Ariga M, Nivean M, Utkarsha P. Pseudoexfoliation Syndrome. *J Curr Glaucoma Pract* 2013; 7(3): 118-120.
2. Sein J, Galor A, Sheth A, et al. Exfoliation syndrome: new genetic and pathophysiologic insights. *Curr Opin Ophthalmol* 2013; 24(2): 167-174.
3. Miglior S, Bertuzzi F. Exfoliative glaucoma: new evidence in the pathogenesis and treatment. *Prog Brain Res* 2015; 221: 233-241.
4. Akarsu C, Unal B. Cerebral haemodynamics in patients with pseudoexfoliation glaucoma. *Eye (Lond)* 2005; 19(12): 1297-1300.
5. Kaya E, Öztürk F. Evaluation of regional brain perfusion in patients with pseudoexfoliation syndrome. *Neuro-Ophthalmology* 2011; 35(5-6): 255-258.
6. Yuksel N, Anik Y, Kilic A, et al. Cerebrovascular blood flow velocities in pseudoexfoliation. *Graefes Arch Clin Exp Ophthalmol* 2006; 244(3): 316-321.
7. Zikou AK, Kitsos G, Astrakas LG, et al. Pseudoexfoliation syndrome without glaucoma: White matter abnormalities detected by conventional MRI and diffusion tensor imaging. *Eur J Radiol* 2018; 99: 82-87.
8. Nucifora PG, Verma R, Lee SK, et al. Diffusion-tensor MR imaging and tractography: exploring brain microstructure and connectivity. *Radiology* 2007; 245(2): 367-384.
9. Chiapponi C, Piras F, Piras F, et al. Cortical grey matter and subcortical white matter brain microstructural changes in schizophrenia are localised and age independent: a case-control diffusion tensor imaging study. *PLoS One* 2013; 8(10): e75115.
10. Jeon T, Mishra V, Uh J, et al. Regional changes of cortical mean diffusivities with aging after correction of partial volume effects. *Neuroimage* 2012; 62(3): 1705-1716.
11. Pfefferbaum A, Adalsteinsson E, Rohlfing T, et al. Diffusion tensor imaging of deep gray matter brain structures: effects of age and iron concentration. *Neurobiol Aging* 2010; 31(3): 482-493.
12. Weston PS, Simpson IJ, Ryan NS, et al. Diffusion imaging changes in grey matter in Alzheimer's disease: a potential marker of early neurodegeneration. *Alzheimers Res Ther* 2015; 7(1): 47.
13. Cercignani M, Inglese M, Pagani E, et al. Mean diffusivity and fractional anisotropy histograms of patients with multiple sclerosis. *AJNR Am J Neuroradiol* 2001; 22(5): 952-958.
14. Della Nave R, Foresti S, Pratesi A, et al. Whole-brain histogram and voxel-based analyses of diffusion tensor imaging in patients with leukoaraiosis: correlation with motor and cognitive impairment. *AJNR Am J Neuroradiol* 2007; 28(7): 1313-1319.
15. Just N. Improving tumour heterogeneity MRI assessment with histograms. *Br J Cancer* 2014; 111(12): 2205-2213.
16. Pope WB, Qiao XJ, Kim HJ, et al. Apparent diffusion coefficient histogram analysis stratifies progression-free and overall survival in patients with recurrent GBM treated with bevacizumab: a multi-center study. *J Neurooncol* 2012; 108(3): 491-498.
17. Tofts PS, Davies GR, Dehmehki J. Histograms: Measuring subtle diffuse disease. In: Tofts PS (ed). *Quantitative MRI of the brain: Measuring changes caused by disease*. John Wiley & Sons, Ltd 2004, pp 581-610.
18. Welsh RC, Rahbar H, Foerster B, et al. Brain diffusivity in patients with neuropsychiatric systemic lupus erythematosus with new acute neurological symptoms. *J Magn Reson Imaging* 2007; 26(3): 541-551.
19. Pierpaoli C, Barnett A, Pajevic S, et al. Water diffusion changes in Wallerian degeneration and their dependence on white matter architecture. *Neuroimage* 2001; 13(6 Pt 1): 1174-1185.
20. Figueroa-Vega N, Moreno-Frias C, Malacara JM. Alterations in adhesion molecules, pro-inflammatory cytokines and cell-derived microparticles contribute to intima-media thickness and symptoms in postmenopausal women. *PLoS One* 2015; 10(5): e0120990.
21. Lee DH, Park JW, Park SH, et al. Have you ever seen the impact of crossing fiber in DTI?: Demonstration of the corticospinal tract pathway. *PLoS One* 2015; 10(7): e0112045.
22. Roescher N, Tak PP, Illei GG. Cytokines in Sjogren's syndrome: potential therapeutic targets. *Ann Rheum Dis* 2010; 69(6): 945-948.
23. Yang P, Gao Z, Zhang H, et al. Changes in proinflam-

- matory cytokines and white matter in chronically stressed rats. *Neuropsychiatr Dis Treat* 2015; 11: 597-607.
24. Oouchi H, Yamada K, Sakai K, et al. Diffusion anisotropy measurement of brain white matter is affected by voxel size: underestimation occurs in areas with crossing fibers. *AJNR Am J Neuroradiol* 2007; 28(6): 1102-1106.
 25. Schmahmann JD, Smith EE, Eichler FS, et al. Cerebral white matter: neuroanatomy, clinical neurology, and neurobehavioral correlates. *Ann N Y Acad Sci* 2008; 1142: 266-309.
 26. Rollins N, Reyes T, Chia J. Diffusion tensor imaging in lissencephaly. *AJNR Am J Neuroradiol* 2005; 26(6): 1583-1586.
 27. Kwee RM, Kwee TC. Virchow-Robin spaces at MR imaging. *Radiographics* 2007; 27(4): 1071-1086.
 28. Pollock H, Hutchings M, Weller RO, et al. Perivascular spaces in the basal ganglia of the human brain: their relationship to lacunes. *J Anat* 1997; 191(Pt 3): 337-346.
 29. Ryan NS, Keihaninejad S, Shakespeare TJ, et al. Magnetic resonance imaging evidence for pre-symptomatic change in thalamus and caudate in familial Alzheimer's disease. *Brain* 2013; 136(Pt 5): 1399-1414.
 30. McLaren ME, Szymkowicz SM, O'Shea A, et al. Vertex-wise examination of depressive symptom dimensions and brain volumes in older adults. *Psychiatry Res Neuroimaging* 2017; 260: 70-75.
 31. Cumurcu T, Cumurcu BE, Celikel FC, et al. Depression and anxiety in patients with pseudoexfoliative glaucoma. *General Hosp Psychiatry* 2006; 28(6): 509-515.
 32. Hamani C, Mayberg H, Stone S, et al. The subcallosal cingulate gyrus in the context of major depression. *Biol Psychiatry* 2011; 69(4): 301-308.
 33. Alexander L, Clarke HF, Roberts AC. A focus on the functions of Area 25. *Brain Sci* 2019; 9(6): 129.



READY-MADE
CITATION

Gkizas CV, Astrakas LG, Zikou AK, Xydis VG, Kitsos G, Argyropoulou MI. Pseudoexfoliation syndrome: Gray matter volume and microstructural changes revealed by histogram and brain surface analysis. *Hell J Radiol* 2020; 5(3): 20-29.